

DESTABILIZATION OF THE ZHANG–RICE SINGLET AT OPTIMAL DOPING

*D. K. Sunko**

*Department of Physics, Faculty of Science, University of Zagreb
HR-10000, Zagreb, Croatia*

Received November 10, 2008

The construction of the Zhang–Rice singlet is revisited in the light of the recent understanding of high-temperature superconductors at optimal doping. A minimal local model is derived that contains the physical regime found relevant for ARPES experiments and characterized by significant direct oxygen–oxygen hopping. For the values of orbital parameters indicated by experiment, the Zhang–Rice singlet is strongly mixed with a pure oxygen singlet of the same symmetry. The Zhang–Rice ground state is destabilized because the coherence factor of the oxygen singlet with respect to oxygen–oxygen hopping is twice as large. An analogous quantum phase transition is identified in the t – t' – J model. The orbital-antisymmetric copper–oxygen singlet is confirmed to be irrelevant, as found originally. The usual symmetry analysis is extended to include dynamical symmetries.

PACS: 74.72.-h, 74.25.Jb, 71.10.Hf

1. INTRODUCTION

The nature of the electron wave functions that undergo the transition to superconductivity in copper-oxide perovskites is still unknown. It is generally assumed, tacitly at least, that the superconducting (SC) transition at optimal doping does not invoke states radically different from those already present at the Fermi level slightly above T_c . In this approach, shared here, the understanding of the normal state is considered the key to the SC mechanism.

The antiferromagnetic (AF) instability in the vicinity of half-filling in the same compounds is by contrast well understood [1] as a charge-transfer effect, dominating the first (large Mott–Hubbard interaction U_d) Coulomb correction [2] to the ideal (paramagnetic) Mott insulator [3]. Theoretical attempts to relate this underdoped region to the SC region on the hole-doped side abound in the literature. They have received early support in the ionic limit by the Zhang–Rice [4] construction, which considered an added hole in an AF background, when double occupation of the copper site was blocked by a large U_d . It is known that the hole then occupies the oxygen sites, each bridging two copper atoms in the CuO_2 plane. Assuming that the

hole prefers to bind with one of the copper atoms, Zhang and Rice have shown that a uniform spreading of the hole around that atom, in an orbitally symmetric “Zhang–Rice singlet” (ZRS) is energetically strongly preferred and propagates like a projected fermion. This provided a way to vindicate the single-band t – J model as a physical reduction of the Emery (three-band Hubbard) model [5, 6], at least for underdoped systems, as an alternative to the usual formal derivation, in which the Foldy–Wouthuysen transformation is applied to the one-band Hubbard model [7].

Challenges to this picture come from two directions. One is fundamental: there is no *a priori* reason for the hole to prefer one copper atom over another. When it is undecided, triplet states are strongly admixed, while it may still move as a fermion [8]. The other challenge is to accept the basic idea of a single CuO_4 molecule, but consider additional states and overlaps within it in order to find the limits of the particular construction used [9]. In the present paper, the natural next step in the Zhang–Rice construction is taken, with just one additional singlet introduced that occupies the oxygen sites.

As is shown below, such an extension is the minimal model that allows expressing the low-energy physics of optimally doped high- T_c superconductors in the small-cluster language. At optimal doping, the Zhang–Rice

*E-mail: dks@phy.hr

ground state becomes strongly admixed with the oxygen singlet chosen by the same symmetry arguments as originally used in [4].

The simplicity of the calculation is used as an opportunity to introduce a classification of state vectors by dynamical symmetry in a small example. This method may have some potential for larger problems.

2. PHYSICAL SCALES

Quantum chemical calculations on small clusters predict the regime

$$U_d \gg \Delta_{pd} > |t_{pd}| \gg |t_{pp}|, \quad (1)$$

used by Zhang and Rice and confirmed in X-ray photoelectron spectroscopy (XPS) experiments [12]. Here, $\Delta_{pd} = \varepsilon_p - \varepsilon_d$ is the copper–oxygen splitting, positive in the hole picture, and t_{pd} and t_{pp} are respectively the copper–oxygen and oxygen–oxygen overlaps. In the limit assumed in (1), the ZRS is the ground state. The energy scale of the XPS experiments and corresponding calculations is 5–10 eV. In high- T_c materials, there is a universally acknowledged crossover scale of the order of 0.1 eV between the lowest and higher energies, although it is still debated whether its origin is phononic [13] or magnetic [14]. Neither small-cluster nor local density approximation (LDA) calculations yield this crossover, and the latter are consistent with the high-energy result in (1).

A recent analysis [15] showed three distinct many-body scales in bismuth strontium calcium copper oxide (BSCCO) that were not reproduced by contemporary LDA calculations, the lowest of which was the above-mentioned crossover, the middle the so-called “waterfall,” not of interest here, and the highest an “anomalous enhancement” of the LDA-predicted bandwidth by about 0.8 eV visible below ε_F in optimally doped BSCCO, i.e., roughly twice that in full. In principle, LDA calculations are able to reach lower energy scales than small-cluster calculations. So far, no *ab initio* effort has reached the vicinity of the Fermi level in high- T_c superconductors. Below the crossover scale, the physical regime of the electrons actually undergoing the transition to superconductivity must still be inferred from phenomenological analysis of low-energy experiments.

The optimally doped region is equally well connected to the metallic overdoped region as to the underdoped one. Attempts to understand the high- T_c perovskites at optimal doping starting from the paramagnetic metal have a long standing on the hole-doped

side [10]. They have mostly been framed in terms of the mean-field slave-boson (MFSB) formalism, allowing effective multiband approaches in which the values of the orbital parameters depart significantly from those expected on the basis of high-energy experiments and LDA calculations [11].

Instead of taking the high-energy “bare” regime as the starting point and introducing many-body effects to reach lower energies, the MFSB phenomenology goes in the opposite direction. Beginning with unprejudiced zeroth-order fits at the Fermi level, one introduces the minimal perturbation necessary to model the lowest crossover. Such an analysis of angle-resolved photoemission spectroscopy (ARPES) [16] has recently been extended to electron-doped compounds [17] and produced the interesting result that their lowest-energy sector is in a physical regime very similar to that in the hole-doped compounds [16, 18]: a large direct oxygen–oxygen hopping t_{pp} , significantly larger than the effective copper–oxygen hopping t_{pd} , and a bandwidth of the same order as the effective copper–oxygen splitting $\Delta_{pd} > 0$ in the hole picture:

$$U_d \gg 4|t_{pp}| \gtrsim \varepsilon_p - \varepsilon_d \equiv \Delta_{pd} \gg \frac{t_{pd}^2}{\Delta_{pd}}. \quad (2)$$

The ARPES scales on which this observation is based are 0.2 eV in BSCCO and 0.5 eV in neodymium cerium copper oxide (NCCO). The lowest-energy crossover was modeled by a (π, π) boson, whose scales were associated with AF in the same compounds. Low-energy regime (2), markedly different from (1), is characterized in particular by an “anticrossing” of the wide oxygen band with the copper level, such that the Fermi level is found in the oxygen-dominated strongly dispersive part of the Brillouin zone, even though $\varepsilon_d < \varepsilon_p$. As we now show, a directly analogous regime exists in the ionic limit.

3. MODEL AND TECHNIQUE

The Hamiltonian of a single CuO_4 molecule is

$$\begin{aligned} H = & \varepsilon_d \sum_{\sigma} \hat{n}_{d\sigma} + \varepsilon_p \sum_{\sigma, i=1}^4 \hat{n}_{p,i\sigma} + \\ & + t_{pd} \sum_{\sigma} (d_{\sigma}^{\dagger} P_{\sigma} + P_{\sigma}^{\dagger} d_{\sigma}) + U_d \hat{n}_{d\uparrow} \hat{n}_{d\downarrow} + \\ & + t_{pp} \sum_{\sigma} \left(p_{+\hat{x},\sigma}^{\dagger} p_{+\hat{y},\sigma} + p_{-\hat{x},\sigma}^{\dagger} p_{-\hat{y},\sigma} + \text{c.c.} \right) - \\ & - t_{pp} \sum_{\sigma} \left(p_{-\hat{x},\sigma}^{\dagger} p_{+\hat{y},\sigma} + p_{-\hat{y},\sigma}^{\dagger} p_{+\hat{x},\sigma} + \text{c.c.} \right), \quad (3) \end{aligned}$$

where

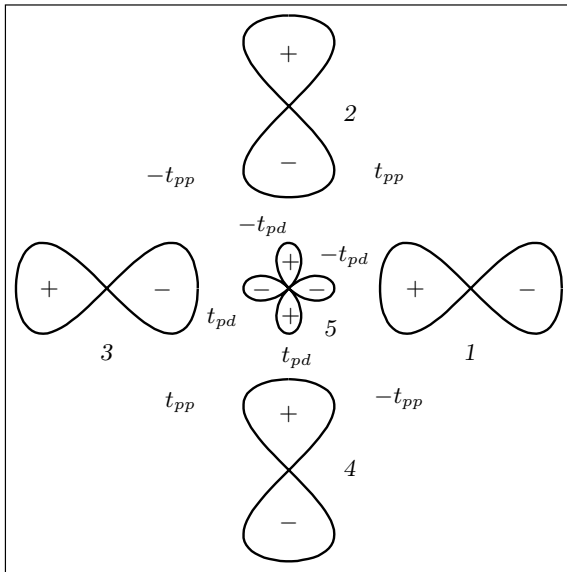


Fig. 1. Orbital parameters and symmetries used in this paper. With our sign convention, $t_{pp} < 0$ is physical [19]

$$P_\sigma = p_{-\hat{x},\sigma} + p_{-\hat{y},\sigma} - p_{+\hat{x},\sigma} - p_{+\hat{y},\sigma}$$

describes the four oxygen atoms around the copper atom, and $\hat{n}_{d\sigma}$ and $\hat{n}_{p,i\sigma}$ are the number operators of the copper and oxygen orbitals. The relevant orbitals and parameters [19] are shown in Fig. 1. All 25 states of two holes with opposite spins on the five orbitals are taken into account.

Standard symmetry analysis is used to reduce Hamiltonian (3) to a block-diagonal form. The basic symmetry is that of the square, corresponding to the group D_4 . We take the z axis, orthogonal to the molecular plane, to be the spin quantization axis. Because the spins have total projection zero, flipping all spins is a symmetry operation, and because all orbitals are planar, this is equivalent to a reflection in the plane. Then D_{4h} is the magnetic (color) group of the problem, and both the ZRS $|ZR\rangle$ and the doubly-occupied copper state $|d^8\rangle$ fall in the A_{1u} representation of D_{4h} , containing five singlets.

As usual, the main symmetry group does not fix the state vectors completely. It is easy to complete the reduction by hand, but instructive to identify the reasons for the remaining ambiguities. One is, as expected, the symmetry under a subgroup, $D_{2h} \subset D_{4h}$. The particular D_{2h} group involved contains the spin-flip operation and three 180° rotations, about the z axis and about the two diagonals at $\pm 45^\circ$ relative to the Cu–O axes. This group stands out because its operations change

the sign of the copper–oxygen overlap t_{pd} , while the energies depend only on t_{pd}^2 .

The more interesting reason is the dynamical symmetry imposed by the assumed degeneracy of the four oxygen orbitals. It eventually affects only two B_{1u} vectors, but to fix them “honestly,” the full dynamical symmetry apparatus must be invoked, even on such a small problem as the present one. The group elements are the Hamiltonian terms that break the oxygen degeneracy. Two are visible in (3), proportional to $+t_{pp}$ and $-t_{pp}$. If these are represented by matrices in the one-particle space, multiplying them generates the third, which corresponds physically to next-to-nearest-neighbor hops from one oxygen atom to another on the same axis. These three elements (and the identity) form the Abelian group D_2 , appearing here as a dynamical symmetry group. The next-nearest-neighbor term must be diagonalized simultaneously with the sum of t_{pp} terms in (3) to separate the last vector without manual intervention.

The outstanding physical feature of dynamical symmetries is that they can connect states with doubly and singly occupied degenerate sites, which is obviously impossible by geometrical transformations. Two technical advantages of dynamical over geometrical symmetry groups are that they increase with the size of the problem, and depend not on shape but on topology. Both are significant when the clusters are motivated by solid-state investigations, and contain many equivalent sites. For example, the dynamical group of the four oxygen atoms in the two-particle space is Z_2^4 , with sixteen elements, which is again Abelian. It is not needed here because the geometrical symmetry already reduces the problem to very small blocks. On the other hand, as a molecule becomes larger, the blocks due to the dynamical symmetry are expected to become smaller than those selected by the geometrical symmetry, especially if the molecule is of odd shape, as is common in Monte Carlo calculations.

4. RESULTS

The complete reduction gives ten stationary states unaffected by t_{pd} . In addition, the Hamiltonian contains six 2×2 blocks and one 3×3 block. The latter is found in the A_{1u} subspace, connecting the states $|d^8\rangle$, $|ZR\rangle$, and the oxygen two-hole singlet

$$|p^{-2}\rangle = \frac{1}{4} (|1\rangle + |2\rangle + |3\rangle + |4\rangle + |12\rangle - |13\rangle - |14\rangle - |23\rangle - |24\rangle + |34\rangle), \quad (4)$$

where

$$|i\rangle = |i\uparrow\rangle|i\downarrow\rangle$$

are doubly occupied states and

$$|ij\rangle = |i\uparrow\rangle|j\downarrow\rangle - |i\downarrow\rangle|j\uparrow\rangle$$

are antisymmetrized singly occupied states. The numbers 1–4 refer to the four oxygens, as in Fig. 1. The block is given by

$$\begin{pmatrix} |d^8\rangle : & 2\varepsilon_d + U_d & 2\sqrt{2}t_{pd} & 0 \\ |ZR\rangle : & 2\sqrt{2}t_{pd} & \varepsilon_d + \varepsilon_p + 2t_{pp} & 2\sqrt{2}t_{pd} \\ |p^{-2}\rangle : & 0 & 2\sqrt{2}t_{pd} & 2\varepsilon_p + 4t_{pp} \end{pmatrix}. \quad (5)$$

The states $|p^{-2}\rangle$ and $|d^8\rangle$ have an equally large coherence factor $2\sqrt{2}t_{pd}$ with respect to $|ZR\rangle$, as found in the perturbation theory [4]. But the coherence factor of the oxygen–oxygen overlap t_{pp} for $|p^{-2}\rangle$ is twice as large as for $|ZR\rangle$. Since the physical sign of t_{pp} is negative, this is a generic mechanism to destabilize the ZRS for all values of U_d (including $U_d \rightarrow \infty$), and hence $|p^{-2}\rangle$ is a relevant perturbation of the Zhang–Rice ground state.

By the same analysis, the orbital-antisymmetric singlet $|OA\rangle$, also considered by Zhang and Rice, appears in a 2×2 B_{1u} block with another oxygen singlet, denoted here by $|pp\rangle$:

$$\begin{pmatrix} |OA\rangle : & \varepsilon_d + \varepsilon_p - 2t_{pp} & 2t_{pd} \\ |pp\rangle : & 2t_{pd} & 2\varepsilon_p \end{pmatrix}. \quad (6)$$

The splitting here is also $\Delta_{pd} + 2t_{pp}$, as between $|p^{-2}\rangle$ and $|ZR\rangle$ in (5), but it occurs because the copper–oxygen singlet is antibonding ($t_{pp} < 0$), while the oxygen singlet is nonbonding with respect to t_{pp} . Its structure is

$$|pp\rangle = \frac{1}{2\sqrt{2}} (-|1\rangle + |2\rangle - |3\rangle + |4\rangle + |13\rangle - |24\rangle). \quad (7)$$

The orbital-antisymmetric state remains irrelevant in the presence of oxygen–oxygen hopping. The t_{pd} -coherence factors in (5) and (6) may be identified by the perturbation theory [4], without the need to distinguish between $|p^{-2}\rangle$ and $|pp\rangle$. However, once t_{pp} is introduced, the different effects on $|ZR\rangle$ and $|OA\rangle$ are related to the different symmetry properties of $|p^{-2}\rangle$ and $|pp\rangle$. The ZRS $|ZR\rangle$ is destabilized because $|p^{-2}\rangle$ has a large coherence factor $4t_{pp}$, while $|OA\rangle$ moves upwards “out of the way,” and $|pp\rangle$ cannot influence the ground state because it is unaffected by t_{pp} (but of course it can anticross with $|OA\rangle$ as that state rises).

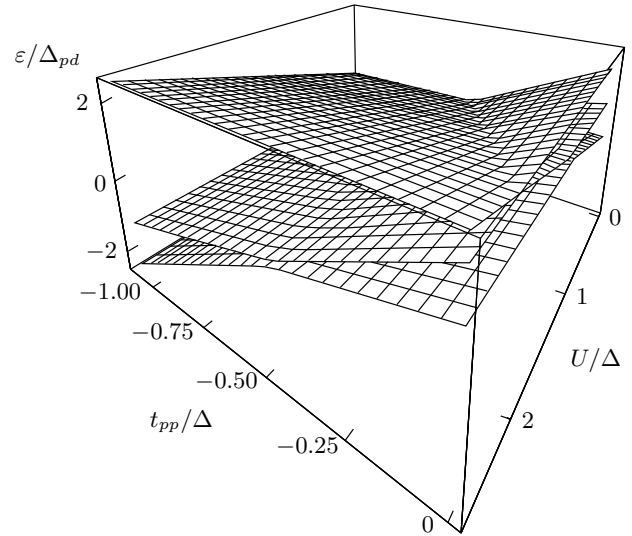


Fig. 2. Parameter space of model (5)

The coherence factors in the reduced model in (5) are the largest in the whole space, and it therefore contains the ground state for $|t_{pd}| \neq 0$ and $t_{pp} < 0$. The relevant parameters are U_d/Δ_{pd} and t_{pp}/Δ_{pd} . The precise value of t_{pd} is irrelevant, as long as parameter regime (2) holds, corresponding to optimal doping. Choosing a low t_{pd} value for graphical reasons, we obtain Fig. 2. At the origin ($U_d = 0$, $t_{pp} = 0$), the weak-coupling regime holds, where the ground state is dominated by $|d^8\rangle$. As U_d increases, this state goes through two anticrossings with the others, and eventually becomes the highest state in the Zhang–Rice regime (U_d large, $|t_{pp}|$ small), where $|ZR\rangle$ is the ground state. As $|t_{pp}|$ increases, the state $|p^{-2}\rangle$ goes down at twice the rate of $|ZR\rangle$, and hence it must eventually anticross with it. Therefore, when both U_d and $|t_{pp}|$ are large, the ZRS is no longer the ground state.

5. DISCUSSION

The present paper describes a simple and robust symmetry-based mechanism that prevents the isolation of the ZRS as the only candidate for the ground state of the CuO_4 ion when U_d is large. Specifically, if the oxygen–oxygen hopping t_{pp} is significant, the local environment is in a charge transfer regime involving two states, the ZRS and an oxygen singlet. The two are mixed by the symmetry-enhanced overlap $2\sqrt{2}t_{pd}$ across the symmetry-reduced gap $\Delta_{pd} + 2t_{pp}$. This is the “metallic” counterpart of the result in [1] that the

antiferromagnetic interaction J near half-filling is also dominated by the charge-transfer term t_{pd}^4/Δ_{pd}^3 , while the Mott–Anderson contribution t_{pd}^2/U is negligible.

It has long been established that ARPES fits require significant ratios of $|t_{pp}/t_{pd}|$ in order to agree with the data [11]. Recent detailed ARPES fits agree with experiment both qualitatively and quantitatively, in practically the same orbital regime for NCCO [17] and BSCCO [16]. The anticrossing regime in (2) is thereby established as an appropriate phenomenology for these compounds, meaning the ratio $|t_{pp}|/\Delta_{pd}$ is also enhanced, especially on the electron-doped side.

Changes in orbital parameters as a function of doping are a standard feature of effective theories, such as the MFSB theory, which account for the effects of strong correlations by changing t_{pd} and Δ_{pd} . The question, as always with effective band models, is what this means for the local environment: Do local hops “see” the bare or the renormalized band parameters? The conclusion that the effective band regime at optimal doping is reflected in an analogous local regime, which implies the destabilization of the ZRS by the above symmetry mechanism, is supported by two independent arguments, one phenomenological and one theoretical.

The recently emphasized [15] failure of LDA calculations to reproduce experimentally observed band widths is phenomenologically significant because LDA predicts a smaller width than is actually observed, and hence any conceivable inclusion of additional correlations would only make the discrepancy larger. Notably, LDA calculations agree with high-energy experiments and calculations in the ionic limit. The anomalous enhancement of hopping via the oxygen sites is consistent by symmetry with the observed discrepancy, which is large in the nodal direction, where the oxygen band is strongly dispersive. The enhancement of the ARPES bandwidth of 1–2 eV over the LDA predictions [15] is quantitatively in good agreement with the value of t_{pp} needed to enter the anticrossing regime, i.e., destabilize the ZRS.

Theoretically, the parameter space of the three-band MFSB model has been extensively investigated [18] from the standpoint of outcomes, namely, which regions of renormalized orbital parameters are indicative of strong renormalization of the input parameters by the MFSB mechanism, and which imply preservation of the bare parameters. In the so-called “resonant-band” regime, characterized by a narrow effective bonding band and copper-dominated wave functions, the quasiparticle weight in the conduction band is significantly reduced, being proportional to the doping δ instead of the total hole content $1 + \delta$.

In that case, the band calculations cannot be directly related to a local picture, since the doped-hole weight is locally either one or zero. But in anticrossing regime (2), the opposite occurs: MFSB theories with Gaussian fluctuations depart from the resonant-band regime and acquire a full quasiparticle weight in the Brillouin zone, only with a reduced t_{pd} [18]. They are therefore comparable and consistent with the present ionic models, as long as both are in the anticrossing limit. The present work therefore reaffirms the possibility [20] that the optimizations leading to a large direct oxygen–oxygen overlap below the crossover scale occur already at the local orbital level.

Realistically, t_{pd} is not so small, and hence the ground state in real materials retains substantial copper content. In the local picture, this means a significant ZRS content in the ground state. However, even if t_{pd} is as large as $|t_{pp}|$, giving a large anticrossing gap of the order of Δ_{pd} , the ground state still contains nearly equal components of $|ZR\rangle$ and $|p^{-2}\rangle$. The system is physically in the charge-transfer regime, which also provides the leading contribution to J [1]. In that case, the reduction to one band by taking the limit [4]

$$\Delta_{pd} = U_d - \Delta_{pd} \rightarrow \infty$$

is purely formal, since that limit forcibly replaces the charge-transfer regime by the Mott regime.

While the MFSB calculations allow regimes with both strong renormalization and no renormalization [18], the derivation of the t – J model from the ZRS [4] implies by construction that the band parameters are locally relevant. However, it has been noted [9] that in order to face experiment, the t – J model needs to be supplemented by additional next- and next-next-to-nearest-neighbor hops, making up the so-called t – t' – t'' – J model. Since the t' term breaks the particle–hole symmetry in the same way as the t_{pp} term in the three-band model, its appearance in practical calculations [21] is immediate evidence that the oxygen degree of freedom cannot be eliminated from the physical picture near optimal doping. The need to introduce t' at the band level translates microscopically into the need to admix oxygen singlet (4) to the ZRS in order to describe the local electronic environment around optimal doping. (When the oxygen is treated explicitly in the band picture, t_{pp} has the same sign for both n - and p -doping [16, 17], as also found in LDA calculations [22], consistently with its simple chemical interpretation.)

To see the real effect of the t' term, the dispersion of the t and t' terms can be rewritten as

$$\begin{aligned}
& -2t(\cos k_x + \cos k_y) - 4t' \cos k_x \cos k_y = \\
& = -4(t + t') + 4(t + 2t') \left(\sin^2 \frac{k_x}{2} + \sin^2 \frac{k_y}{2} \right) - \\
& \quad - 16t' \sin^2 \frac{k_x}{2} \sin^2 \frac{k_y}{2}, \quad (8)
\end{aligned}$$

separating contributions by the particle–hole symmetry. The second term is manifestly symmetric around half-filling, while the third is not, since it achieves its minimum value (zero) along the nondispersive lines $k_x = 0$ and $k_y = 0$. In practice, $tt' < 0$ and the ratio $|t'/t| \approx 0.2\text{--}0.4$. For $t' = -0.3t$, which is a common enough parameterization around optimal doping,

$$\left| \frac{4t'}{t + 2t'} \right| = 3,$$

and hence the symmetry-breaking term enters with three times the contribution of the symmetry-preserving term. The apparently small values of $|t'/t|$ found in the literature are therefore quite misleading in terms of the actual amount of particle–hole symmetry breaking needed to achieve realistic Fermi surface fits within the $t\text{--}t'\text{--}J$ model. In particular, for $t' = -t/2$, the symmetry-preserving term vanishes and the $t\text{--}t'\text{--}J$ model passes through a quantum phase transition in the vicinity of its applicable parameter range.

By symmetry, this is the same type of transition appearing in the present paper as the destabilization of the ZRS in the three-band case. Physically, they are different insofar as the three-band model destabilizes the ZRS by oxygen hopping in a low order, while in the $t\text{--}t'\text{--}J$ model, the ZRS are preserved by assumption and the transition occurs by the additional t' overlap among them, i.e., in a high order in the original three-band model. But as regards accounting for ARPES data, both models agree in that such a transition is approached near optimal doping.

The limitation of the above arguments to the metallic phase should be kept in mind. Near half-filling, the oxygen hopping is effectively reduced by the antiferromagnetic interactions, and the system is insulating precisely at half-filling independently of the value of t_{pp} . In the insulating phase, the high-energy ionic limit is recovered, both theoretically and experimentally. As t_{pp} becomes more effective with doping, locally the first admixture to the ZRS appears, identified here as oxygen singlet (4). A broad picture of the optimal-doping regimes of high- T_c compounds thus emerges, in which NCCO is deep in the anticrossing regime, $4|t_{pp}| \gg \Delta_{pd}$, and BSCCO is at its limit, $4|t_{pp}| \approx \Delta_{pd}$. On the other hand, the remarkable Fermi-surface evolution of lanthanum strontium copper oxide (LSCO) with doping [23] is indicative of strong renormalizations of the

band parameters, especially when the system is underdoped. In such a resonant-band regime, it was also shown directly [24] that the strong doping dependence of t_{pp} in the MFSB fits does not imply a similar variation of the local parameters.

The present analysis points to one pitfall of considering the oxygen part of the ZRS as a single-particle state in its own right, as if the hole on the copper atom were unhybridized with the oxygen atoms. However, the same caution applies to the oxygen singlet found here. In particular, one should be careful in interpreting the corresponding Bloch states. The propagation of strongly correlated cluster states in a lattice in more than one dimension is at present largely unexplored, with controlled analytic results available only in special limits, which themselves amount to uncontrolled simplifications. Such is the limit of infinite dimensions [25], physically corresponding to diffusion, or the Falicov–Kimball limit [26], which is dispersive, but replaces dynamical constraints by geometrical ones.

The model presented here is as sparse as possible, allowing the experimentally observed regime with only three state vectors. To avoid being too minimal, we should give some attention to the neglected Coulomb integrals U_p , V_{pp} , and V_{pd} , which are respectively the on-site oxygen, intracell oxygen, and copper–oxygen repulsions. They do not break the symmetries above, introducing only matrix elements within each symmetry block. In particular, they connect the ground-state block in (5) with the other two A_{1u} states by matrix elements $U_p/4$, which are smaller than the terms $2\sqrt{2}t_{pd}$. On the diagonal of this block, the Coulomb terms can be reabsorbed into site energies and the copper on-site repulsion U_d . For realistic $V_{pp} \ll U_p$, this leads to a small reduction in the copper–oxygen splitting Δ_{pd} , and practically no change in U_d , while for large $V_{pp} = U_p/2$, a useful limit case, the effective U_d increases and the effective Δ_{pd} decreases, both by about 1 eV. Hence, the inclusion of neglected integrals mildly tends to push the system further into the anticrossing $U_d \rightarrow \infty$ regime.

An extension of the Zhang–Rice argument to the electron-doped side is only possible with larger molecules, containing more than one copper atom. This would allow studying the competition of magnetic and charge ordering at the local level. It also opens a way to compare the Zhang–Rice and Emery–Reiter [8] constructions directly on the hole-doped side. Obviously, the spaces involved are much larger. It is on these larger problems, both theoretical and numerical, that hope is invested in the assignment of quantum numbers

by dynamical symmetries, as introduced in the present work.

6. CONCLUSION

It has been found that in the presence of local repulsion on copper atoms, the direct oxygen–oxygen overlap is a relevant perturbation of the Zhang–Rice singlet. With the possible exception of LSCO, real hole- and electron-doped high- T_c superconductors appear to be in a physical regime where the Zhang–Rice singlet is strongly mixed with a pure oxygen singlet.

Conversations with S. Barišić are gratefully acknowledged. This work was supported by the Croatian Government under Project 119-1191458-0512.

REFERENCES

1. H. Eskes and J. H. Jefferson, *Phys. Rev. B* **48**, 9788 (1993).
2. P. W. Anderson, *Phys. Rev.* **115**, 2 (1959).
3. N. F. Mott, *Proc. Phys. Soc. A* **62**, 416 (1949).
4. F. C. Zhang and T. M. Rice, *Phys. Rev. B* **37**, 3759 (1988).
5. V. J. Emery, *Phys. Rev. Lett.* **58**, 2794 (1987).
6. C. M. Varma, S. Schmitt-Rink, and E. Abrahams, *Sol. St. Comm.* **62**, 681 (1987).
7. P. Fulde, *Electron Correlations in Molecules and Solids*, Springer (1993).
8. V. J. Emery and G. Reiter, *Phys. Rev. B* **38**, 11938 (1988).
9. A. M. Macridin, M. Jarrell, T. Maier, and G. A. Sawatzky, *Phys. Rev. B* **71**, 134527 (2005).
10. G. Kotliar, P. A. Lee, and N. Read, *Physica C* **153–155**, 538 (1988).
11. Qimiao Si, Yuyao Zha, K. Levin, and J. P. Lu, *Phys. Rev. B* **47**, 9055 (1993).
12. M. A. van Veenendaal, G. A. Sawatzky, and W. A. Groen, *Phys. Rev. B* **49**, 1407 (1994).
13. W. S. Lee, S. Johnston, T. P. Devereaux, and Z.-X. Shen, *Phys. Rev. B* **75**, 195116 (2007).
14. T. Valla et al., *Phys. Rev. Lett.* **98**, 167003 (2007).
15. W. Meevasana et al., *Phys. Rev. B* **75**, 174506 (2007).
16. D. K. Sunko and S. Barišić, *Eur. Phys. J. B* **46**, 269 (2005).
17. D. K. Sunko and S. Barišić, *Phys. Rev. B* **75**, 060506(R) (2007).
18. I. Mrkonjić and S. Barišić, *Eur. Phys. J. B* **34**, 69 (2003).
19. D. I. Golosov, A. E. Ruckenstein, and M. L. Horbach, *J. Phys.: Cond. Matt.* **10**, L229 (1998).
20. A. A. Abrikosov and L. A. Fal'kovskii, *JETP Lett.* **49**, 531 (1989).
21. B. Kyung, V. Hankevych, A.-M. Daré, and A.-M. S. Tremblay, *Phys. Rev. Lett.* **93**, 147004 (2004).
22. M. M. Korshunov et al., *Phys. Rev. B* **72**, 165104 (2005).
23. A. Ino et al., *J. Phys. Soc. Jpn.* **68**, 1496 (1999).
24. L. Janković and D. K. Sunko, *Physica C* **341–348**, 2103 (2000).
25. A. Georges, G. Kotliar, W. Krauth, and M. J. Rozenberg, *Rev. Mod. Phys.* **68**, 13 (1996).
26. D. K. Sunko, *Eur. Phys. J. B* **43**, 319 (2005).